Письма в ЭЧАЯ. 2012. Т. 9, № 6–7(176–177). С. 806–813

МЕТОДИКА ФИЗИЧЕСКОГО ЭКСПЕРИМЕНТА

STUDY OF COMPLETE AND INCOMPLETE FUSION FOR LOOSELY BOUND PROJECTILES ^{6}He AND ^{6}Li ON ^{165}Ho AND ^{166}Er TARGETS

A. S. Fomichev [a], *V. Chudoba* [a,b], *A. V. Daniel* [a], *M. S. Golovkov* [a], *V. A. Gorshkov* [a], *S. A. Krupko* [a], *Yu. Ts. Oganessian* [a], *G. S. Popeko* [a], *S. I. Sidorchuk* [a], *R. S. Slepnev* [a], *G. M. Ter-Akopian* [a], *R. Wolski* [a,c], *V. I. Chepigin* [a], *D. E. Katrasev* [a], *O. N. Malyshev* [a], *A. I. Svirikhin* [a], *A. V. Yeremin* [a], *Ch. Briançon* [d], *K. Hauschild* [d], *A. Korichi* [d], *M.-H. Ha* [d], *F. Hanappe* [e], *O. Dorvaux* [f], *L. Stuttge* [f]

[a] Joint Institute for Nuclear Research, Dubna

[b] Institute of Physics, Silesian University in Opava, Czech Republic

[c] The Henryk Niewodniczanski Institute of Nuclear Physics, PAS, Cracow, Poland

[d] CSNSM, IN2P3-CNRS, UMR8609, Orsay, France

[e] Université Libre de Bruxelles, PNTPM, Bruxelles, Belgium

[f] Institut de Recherches Subatomiques, IN2P3/ULP, Strasbourg, France

Complete fusion (CF) and incomplete fusion (ICF) reactions were studied for the cases of the loosely bound ^{6}He and ^{6}Li projectiles bombarding ^{166}Er and ^{165}Ho targets at energy of about 10 MeV/nucleon. Experiments were carried out to test an approach exploiting the measured intensities of γ rays emitted at the transitions between the yrast-band levels of reaction products formed after the termination of neutron evaporation. Partial waves feeding the CF reactions $^{165}\mathrm{Ho}\,(^{6}\mathrm{Li}, 5n)\,^{166}\mathrm{Yb}$ and $^{166}\mathrm{Er}\,(^{6}\mathrm{He}, 6n)\,^{166}\mathrm{Yb}$ as well as ICF $^{165}\mathrm{Ho}\,(^{6}\mathrm{Li}, \alpha 3n)\,^{164}\mathrm{Er}$ and $^{166}\mathrm{Er}\,(^{6}\mathrm{He}, \alpha 4n)\,^{164}\mathrm{Er}$ reaction channels were revealed from the obtained γ-ray data. The method of exit channel identification via the triple coincidence ($\gamma 1 - \gamma 2$–light charged particle) was employed for these reactions study.

Реакции полного и неполного слияния изучались для случаев слабосвязанных снарядов ^{6}He и ^{6}Li, бомбардирующих мишени ^{166}Er и ^{165}Ho при энергии около 10 МэВ/нукл. Эксперименты были сделаны с целью проверки применимости метода измерения относительных интенсивностей гамма-квантов, испущенных при переходах с возбужденных уровней ираст-полосы после завершения процесса испарения нейтронов. Парциальные вклады, свойственные реакциям полного слияния $^{165}\mathrm{Ho}\,(^{6}\mathrm{Li}, 5n)\,^{166}\mathrm{Yb}$ и $^{166}\mathrm{Er}\,(^{6}\mathrm{He}, 6n)\,^{166}\mathrm{Yb}$, так же как и каналам реакций неполного слияния $^{165}\mathrm{Ho}\,(^{6}\mathrm{Li}, \alpha 3n)\,^{164}\mathrm{Er}$ и $^{166}\mathrm{Er}\,(^{6}\mathrm{He}, \alpha 4n)\,^{164}\mathrm{Er}$, были извлечены из полученных данных гамма-спектров. Был использован метод идентификации выходных каналов реакций полного и неполного слияния за счет тройных совпадений ($\gamma 1 - \gamma 2$–легкая заряженная частица), позволяющий изучать эти реакции.

PACS: 25.60.-t; 25.70.Jj; 25.70.Mn

INTRODUCTION

Fusion reactions of loosely bound stable and unstable nuclei, such as ^{6}Li, ^{7}Li and ^{9}Be, and radioactive ^{6}He and ^{11}Be possessing neutron halos, were repeatedly studied both experimentally and theoretically, see reviews in [1–3]. Experiments were mostly designed to measure the CF and ICF reaction cross sections at different projectile energies below and above the Coulomb barrier. Comprehensive measurements of the CF and incomplete fusion (ICF) cross sections were reported in [4] for the $^{6}\mathrm{Li} + {}^{209}\mathrm{Bi}$, $^{7}\mathrm{Li} + {}^{209}\mathrm{Bi}$, and $^{9}\mathrm{Be} + {}^{208}\mathrm{Pb}$ reactions. Besides the observation of the radioactive decay of the product nuclei, which were formed in these reactions, the yields of different evaporation residues could be measured also by detecting either the delayed X rays [5] or characteristic prompt γ rays [6].

As compared with the expectations of single-barrier penetration models and coupled channel calculations, leaving aside couplings to the continuum states, the measured CF cross sections are higher at energies below Coulomb barrier and lower at the above-barrier energies. The CF cross section suppression for weakly bound systems at energies above the barrier implies that a part of the flux expected to feed the CF goes to breakup and, at least, partly manifests itself in the ICF. In this situation, other experimental approaches based on new observables are highly desirable.

We performed experiments aimed to test an approach exploiting the measured intensities of γ rays emitted at transitions between the yrast-band levels of reaction products formed after the termination of neutron evaporation. This seems to be promising for getting access to the spin distributions in the excited nuclei formed in the CF or ICF reactions. As regards the information on the l dependence of transmission coefficients $T_l(E)$, the reliability of this approach was demonstrated in the studies of CF reactions induced by tightly bound nuclei ^{4}He, ^{12}C and ^{16}O on medium mass targets [7, 8].

In light of the quite similar wave functions given for ^{6}He and ^{6}Li by the three-body theory model [9], it will be of special interest to study the reactions induced by the beams of these loosely bound nuclei in comparison with the ^{4}He projectile. Cross sections for the $2n, 3n$ and $4n$ evaporation in the $^{166}\mathrm{Er}\,(^{4}\mathrm{He}, xn)\,^{170-x}\mathrm{Yb}$ reactions were measured and analyzed in [7 and Refs. therein]. So, our interest was focused on the $6n$ and $5n$ evaporation channels in the reactions $^{166}\mathrm{Er}\,(^{6}\mathrm{He}, 6n)\,^{166}\mathrm{Yb}$ and $^{165}\mathrm{Ho}\,(^{6}\mathrm{Li}, 5n)\,^{166}\mathrm{Yb}$ resulting in the same well-known residual nucleus ^{166}Yb. The addition of the $^{6}\mathrm{Li} + {}^{166}\mathrm{Er}$ reaction makes specific interest because in this case one can easily identify the products of the ^{6}Li breakup ending with the capture of its α cluster by ^{166}Er. This is much more difficult to attain in the case of the $^{6}\mathrm{He} + {}^{166}\mathrm{Er}$ reaction because the same products are formed in the complete and partial fusion reactions.

1. EXPERIMENTS

We studied CF and ICF reactions occurring in the collisions of a 64-MeV ^{6}He beam with ^{166}Er and a 58-MeV beam of ^{6}Li ions with ^{165}Ho and ^{166}Er targets. Experiments were carried out at a beam line of the «Dubna Radioactive Ion Beams» facility (DRIBs) [10]. The ion beam (either ^{6}He or ^{6}Li) was focused in a 15-mm spot on the target. The targets were the layers of Er_2O_3 (7.5 mg/cm^2 thick) or Ho_2O_3 (5 mg/cm^2 thick) deposited on 11-μ Al foils. The ^{166}Er isotope was of 95% enrichment in the erbium target. Gamma rays emitted by reaction evaporation residues, stopped in the target or in its backing, were detected by six coaxial, HP

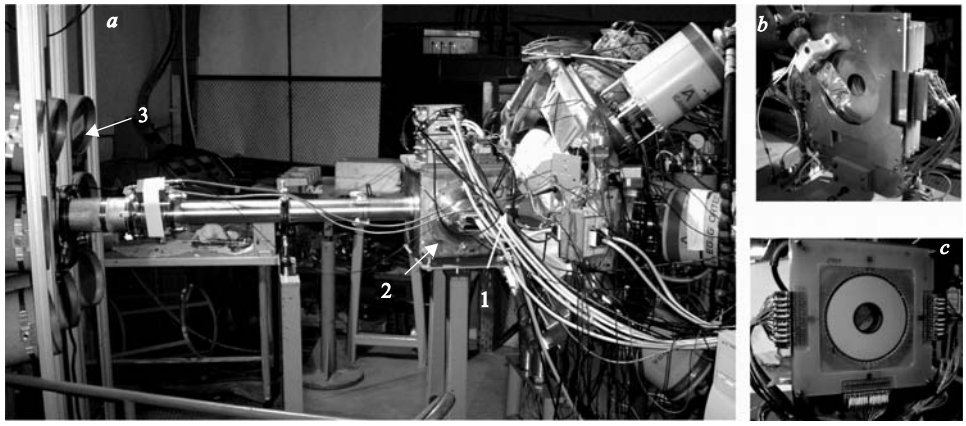

Fig. 1. View of the experimental setup is shown on the panel *a*. The beam comes from the right side. By Arabic numerals are indicated: *1* — target (^{165}Ho or ^{166}Er); *2* — reaction chamber with the detectors inside; *3* — neutron detectors array; *4* — γ detectors array. Panels *b* and *c* show back and front side views of the silicon telescope together with monitor detector respectively installed inside the box in the beam axis downstream from the target

Ge detectors [11] from the French–UK loan pool. Each Ge crystal was surrounded by the BGO Compton suppression array. The BGO crystals were 70 mm in diameter and height and looked at the target from the upstream side and being inclined by 45° towards the beam axis. A distance of 15 cm was set between the target and the front end of each BGO detector. It was a new geometry for the GABRIELA γ-array [12]. An annular telescope composed of one 0.3-mm and two 1-mm Si strip detectors (all with 32 and 82 mm in inner and external diameters, respectively) was used to detect charged particles emitted from the target in forward direction with respect to the beam axis. The first layer was segmented in 16 rings and 16 sectors, while each of the other layers had only one common ring and 8 sectors. The telescope covered a range of polar angle $\theta = 9.5{-}42.0°$. An array of neutron detectors consisting of eight units of the ToF spectrometer DEMON [13] was installed close to zero-angle direction, 1.5 m far from the target. It was used as an auxiliary device to test the detection method suitable for neutrons emitted at the projectile break-ups. The experimental setup is schematically shown in Fig. 1. An additional detector for the beam monitoring consisting of 0.5-mm BC404 plastic coupled with Hamamatsu R1924 PMT was installed on the beam axis downstream from the Si telescope (it is shown in top incision).

Single γ rays with energy $E_\gamma \approx 90$ keV were detected by one Ge module in the full energy absorption peak with probability 1.3%. The detection efficiency dropped to 0.15% at $E_\gamma \approx 1000$ keV. The peak width (FWHM) obtained for 200–500 keV γ rays was about 3.2 keV. Pair coincidences of γ rays detected within a 70-ns time interval triggered data acquisition. The same time was set for the charged particles detected in coincidence with the trigger. An auxiliary trigger used to monitor the beam intensity by the elastically scattered beam nuclei originated from signals taken from the front detector of the charged particle telescope. The beam intensity was maintained at a level of $5 \cdot 10^6$ s^{-1}. In each of the two main runs aimed at the observation of CF and ICF in the $^{166}\mathrm{Er} + {}^{6}\mathrm{He}$ and $^{165}\mathrm{Ho} + {}^{6}\mathrm{Li}$ reactions, the total acquired beam doses made about $2 \cdot 10^{12}$. About the same beam dose was collected in the case of the $^{166}\mathrm{Er} + {}^{6}\mathrm{Li}$ reaction which was used for the ICF observation.

2. RESULTS AND DISCUSSION

Coincidence peaks were revealed in the two-dimensional γ-ray spectra built in the $E_{\gamma 1}$ versus $E_{\gamma 2}$ plane. The count numbers obtained within individual $\gamma-\gamma$ peaks were estimated using the approach presented in [14]. First, we present the data on the ^{166}Yb γ rays detected for the $^{165}\mathrm{Ho} + {}^{6}\mathrm{Li}$ and $^{166}\mathrm{Er} + {}^{6}\mathrm{He}$ reactions.

When holmium was bombarded by ^{6}Li the ^{166}Yb nuclei could be produced only in the $^{165}\mathrm{Ho}\,(^{6}\mathrm{Li}, 5n)\,^{166}\mathrm{Yb}$ reaction. We succeeded to measure intensities for the $\gamma-\gamma$ coincidence peaks corresponding to the γ rays emitted at transitions between the levels of the ^{166}Yb ground-state band and band 8 (according to notations in [15]). This provided direct access to the intensities of γ rays emitted from specific levels of ^{166}Yr. These intensities obtained for the $^{165}\mathrm{Ho}\,(^{6}\mathrm{Li}, 5n)\,^{166}\mathrm{Yb}$ reaction are presented in Fig. 2, *a*.

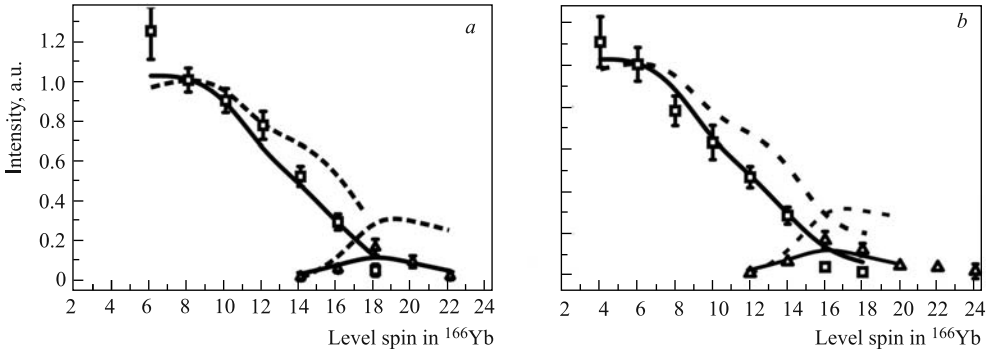

Fig. 2. Relative intensities of ^{166}Yb γ rays emitted from the levels of the ground-state band (squares) and band 8 (triangles). Solid and dashed lines show the results of calculations done with the code EMPIRE [13] (see text). Panels *a* and *b* show the results obtained for the reactions $^{165}\mathrm{Ho}\,(^{6}\mathrm{Li}, 5n)\,^{166}\mathrm{Yb}$ and $^{166}\mathrm{Er}\,(^{6}\mathrm{He}, 6n)\,^{166}\mathrm{Yb}$, respectively

Similar data were obtained for the $^{166}\mathrm{Er} + {}^{6}\mathrm{He}$ reaction where ^{166}Yb was mostly produced as a result of the $6n$ evaporation reaction channel $^{166}\mathrm{Er}\,(^{6}\mathrm{He}, 6n)\,^{166}\mathrm{Yb}$. However, incomplete fusion with the α core of ^{6}He captured by the target nucleus (and the two halo neutrons flying forward as spectators) could contribute in the data observed. We estimated this contribution starting from the intensities of the ^{166}Yb γ rays recorded for the $^{166}\mathrm{Er} + {}^{6}\mathrm{Li}$ reaction. Using the $\gamma-\gamma$ spectrum recorded in coincidence with deuterons and protons, we got the $\gamma-\gamma$ peaks of ^{166}Yb which were free from the background caused by the electron capture decays of the ^{166}Lu isomers which could be formed in the $^{166}\mathrm{Er}\,(^{6}\mathrm{Li}, 6n)\,^{166}\mathrm{Lu}$ reaction. A calculation done with the EMPIRE code [16] made us sure that the effect of the $^{166}\mathrm{Er}\,(^{6}\mathrm{Li}, p5n)$ reaction was negligible. As a result, the effects of the ICF reactions associated with the capture of either the ^{6}Li or ^{6}He α clusters by the ^{166}Er nuclei were estimated to be less than 10% as compared to the intensities of the ^{166}Yb γ rays measured for the $^{165}\mathrm{Ho}\,(^{6}\mathrm{Li}, 5n)\,^{166}\mathrm{Yb}$ and $^{166}\mathrm{Er}\,(^{6}\mathrm{He}, 6n)\,^{166}\mathrm{Yb}$ reactions. The corresponding correction was done for the case of the latter reaction. The so obtained γ-ray intensities for the $^{166}\mathrm{Er}\,(^{6}\mathrm{He}, 6n)\,^{166}\mathrm{Yb}$ reaction are presented in Fig. 2, *b*.

We followed the approach presented in [7, 8] to deduce, relying on the measured intensities of ^{166}Yb γ rays, the spin distributions of the highly excited $^{172}\mathrm{Yb}^{*}$ and $^{171}\mathrm{Yb}^{*}$ compound

nuclei formed in the $^{166}\mathrm{Er} + {}^{6}\mathrm{He}$ and $^{165}\mathrm{Ho} + {}^{6}\mathrm{Li}$ reactions. Calculations were done using the code EMPIRE [16]. Firstly, we took the default mode suggested in this code where the CF cross section is calculated by means of the simplified Coupled-Channels approach [17] (CCFUS code). The spin dependences of the γ-ray intensities that followed from these calculations for the $^{165}\mathrm{Ho}\,(^{6}\mathrm{Li}, 5n)\,^{166}\mathrm{Yb}$ and $^{166}\mathrm{Er}\,(^{6}\mathrm{He}, 6n)\,^{166}\mathrm{Yb}$ reactions are shown with dashed lines in Figs. 2, *a, b*. The poor agreement of these lines with the experimental points is evident. In view of this discrepancy, we carried out calculations in an EMPIRE mode allowing one to obtain the γ-ray intensities by specifying the critical angular momentum l_{cr} and diffuseness parameter D_l. We made χ^2 fits to find the l_{cr} and D_l values resulting from the best fits to the data, see the table. The solid lines in Figs. 2, *a, b* show the spin dependences of the γ-ray intensities obtained from these fits. As a result, we define the suppression factor to the CF cross section as the ratio of the cross section deduced from the obtained l_{cr} and D_l values (column «χ^2 fit to experiment» in the table) to the cross-section value calculated with EMIRE default parameters. The data show obviously that the suppression factor for the $^{166}\mathrm{Er} + {}^{6}\mathrm{He}$ reaction is larger than the value obtained for the $^{165}\mathrm{Ho} + {}^{6}\mathrm{Li}$ case. One could conclude that this meaningful difference reflects the projectile properties from the point of view of the fusion probability. A reasonable assumption is that in the high angular momentum region incomplete fusion and/or break-up became the main reaction channels and it is more preferable for manifestation in the $^{166}\mathrm{Er} + {}^{6}\mathrm{He}$ case.

Results obtained from calculations done with code EMPIRE [16] employing the data of Figs. 2, *a, b*. The ratios of the CF cross-section values obtained as the EMPIRE default results (column 2) and from the χ^2 fits (column 3) are presented in column 4 as the CF suppression factors. Other notations are in text

Reaction / beam energy, MeV	σ_{fus}, mb / l_{cr}, $\hbar$		CF suppression factor	σ_{xn}, mb / D_l, $\hbar$	
	EMPIRE default	χ^2 fit to experiment		EMPIRE default	χ^2 fit to experiment
$^{166}\mathrm{Er}\,(^{6}\mathrm{He}, 6n)$ / 64	2490 / 39.0	731 / 19.3	3.41	881 / 1.5	254 / 1.5
$^{165}\mathrm{Ho}\,(^{6}\mathrm{Li}, 5n)$ / 58	1770 / 32.5	737 / 18.6	2.40	656 / 0.2	244 / 0.4

Specific information could be obtained for ICF in the $^{165}\mathrm{Ho} + {}^{6}\mathrm{Li}$ and ^{166}Er+^{6}He systems. We note that the experimental arrangement provided the observation for the clusters appearing at the projectile break-ups associated with the incomplete fusion process. Energy spectra measured for the detected ^{4}He nuclei are shown in Fig. 3. Notable are their quite narrow widths and the most probable energies consistent with the break-up mechanism. More specific will be to compare these spectra with simulations assuming the projectile break-up, leaving the α cluster to run quasi-free, while another cluster is captured by the target. Such simulations were done with the Hulthén wave function (WF) of deuteron adapted for ^{6}Li. For ^{6}He we used the WF from [18].

It appeared that the «di-neutron» component of the ^{6}He WF resulted in the best fit to the measured spectrum of Figs. 3, *b*. The spectra in Figs. 3, *a, b* testify to the ICF reactions as the source of the recorded ^{4}He nuclei. Evidently, contribution from the transfer reaction mechanism to the intensities of γ rays emitted by such an evaporation residue as is the ^{164}Er formed in the $^{165}\mathrm{Ho}(^{6}\mathrm{Li}, \alpha 3n)$ and $^{166}\mathrm{Er}\,(^{6}\mathrm{He}, \alpha 4n)$ reactions should be vanishing. Besides

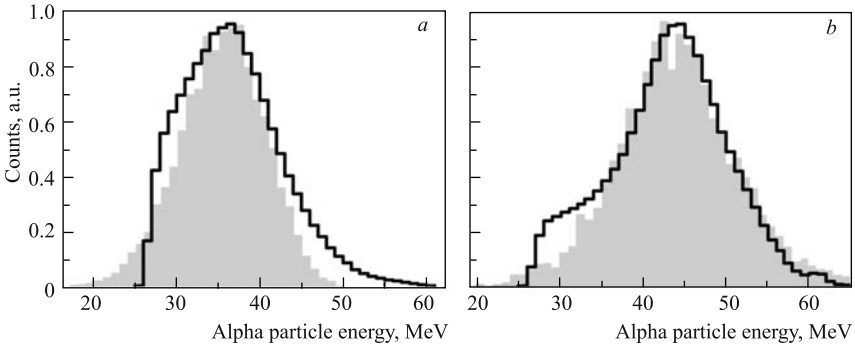

Fig. 3. Energy spectra of ^{4}He nuclei. Thick solid lines in panels a and b show the spectra measured for the $^{165}\mathrm{Ho} + {}^6\mathrm{Li}$ and $^{166}\mathrm{Er} + {}^6\mathrm{He}$ reactions, respectively. The cut-offs seen at about 25 MeV are caused by the lack of α particles stopped in the first, 300 μ telescope detector. Shadowed histograms show the results of simulations (see text)

the comparison between the spectra shown in Figs. 3, *a, b* this is verified by the fact that these $3n$ and $4n$ evaporation reactions require the formation of $^{167}\mathrm{Er}^*$ and $^{168}\mathrm{Er}^*$ nuclei excited to 30–40 and 35–50 MeV, respectively. Hardly, the deuteron or «di-neutron» transfer mechanisms could populate so highly excited states in these nuclei.

The intensities of γ rays emitted from the levels of the ground-state band of ^{164}Er originating from the $^{165}\mathrm{Ho}\,(^6\mathrm{Li}, \alpha 3n)$ and $^{166}\mathrm{Er}\,(^6\mathrm{He}, \alpha 4n)$ reactions are shown in Figs. 4, *a, b*. In view of the small values of critical angular momentum (l_{cr}) obtained for the CF cross section it appeared reasonable to analyze the ^{164}Er data, assuming that the ICF reaction can be characterized by two parameters $l_{\mathrm{cr\,min}}$ and $l_{\mathrm{cr\,max}}$ responsible for the cut-offs occurring on both the small ($l_{\mathrm{cr\,min}}$) and large ($l_{\mathrm{cr\,max}}$) sides of the orbital momentum distributions.

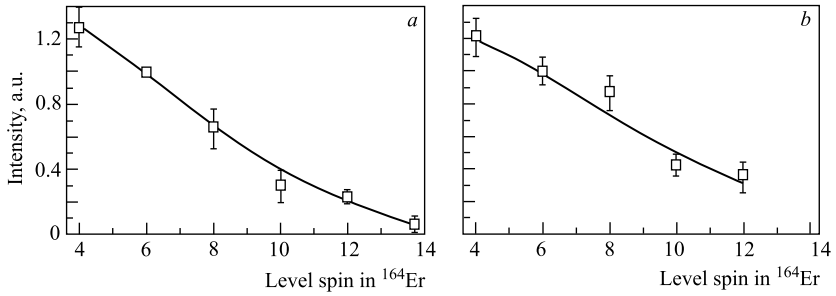

Fig. 4. Relative intensities obtained for the ^{164}Er γ rays emitted from the levels of the ground-state band (the experimental points are presented by squares). Solid lines show the fits done with TALYS [19] (see text). Panels *a* and *b* show data for the reactions $^{165}\mathrm{Ho}\,(^6\mathrm{Li}, \alpha 3n)$ and $^{166}\mathrm{Er}\,(^6\mathrm{He}, \alpha 4n)$, respectively

In the fits done for the ^{164}Er data we approximated the values of these parameters as $l_{\mathrm{cr\,max}} = k_{\max} E^{1/2}$ and $l_{\mathrm{cr\,min}} = k_{\min} E^{1/2}$ and the two parameters, $k_{\max}$ and $k_{\min}$, were fitted. The energy E of the virtual deuteron («di-neutron») captured by the target nucleus followed from the excitation energy of $^{167}\mathrm{Er}^*$ ($^{168}\mathrm{Er}^*$) which, in its turn, was fixed provided that a ^{4}He energy value was selected. The fits were done in series taking different energy bins shown in Fig. 3 and summing the results. Diffuseness parameters were fixed to be $D_{l\,\min} = D_{l\,\max} = 0.5$.

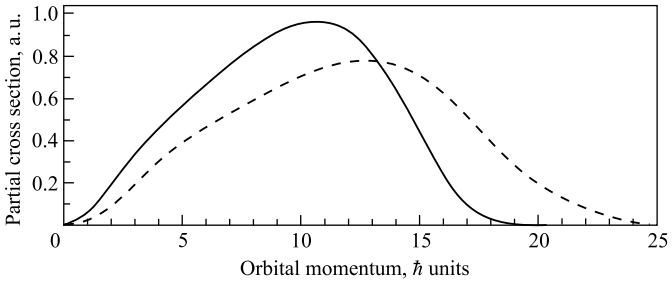

Fig. 5. Partial waves contributions in the ICF cross section feeding reaction channels ^{165}Ho (^{6}Li, $\alpha 3n$) and ^{166}Er (^{6}He, $\alpha 4n$) are shown by the solid and dashed curves, respectively

Intensity distributions obtained from these fits are shown by curves in Figs. 4, *a, b*. From the χ^2 fits we got the following values for the parameters governing the lower and higher orbital momentum cut-offs: $k_{\min} = 0.3$, $k_{\max} = 3.2$ for the case of the ^{165}Ho (^{6}Li, $\alpha 3n$) reaction and $k_{\min} = 0.5$, $k_{\max} = 3.9$ for the reaction ^{166}Er (^{6}He, $\alpha 4n$). Taking these particular values, one comes to the distributions of partial cross sections which contribute to the yields of these ICF reaction channels. These distributions are presented in Fig. 5.

CONCLUSION

In summary we note that the results of these experiments testify to the reasonable conclusions made, within the approach adopted in our work, on the CF cross sections of the loosely bound ^{6}Li and ^{6}He nuclei. Firstly, kinematically complete experiments including the measurement of gammas, neutrons and light charged particles were carried out. The values derived in this work for the CF cross sections are consistent with similar data obtained for the CF reactions in the works where these cross sections were measured in a common way. It has been shown that this approach gives access to the partial wave distributions between the CF and ICF reaction channels. The beam energies were well above the fusion barrier in this work. However, our data show that similar measurements are feasible for the near-barrier and sub-barrier beam energies.

Acknowledgements. The authors are grateful to Prof. S. N. Dmitriev for continuous support of this experiment. This work was supported by the Russian Foundation for Basic Research grants RFBR No. 11-02-00657-a and No. 11-02-00490-a.

REFERENCES

1. *Canto L. F. et al.* // Phys. Rep. 2006. V. 424. P. 1.
2. *Liang J. F., Signorini C.* // Intern. J. Mod. Phys. E. 2005. V. 14. P. 1121.
3. *Keeley N. et al.* // Prog. Part. Nucl. Phys. 2007. V. 59. P. 579.
4. *Dasgupta M. et al.* // Phys. Rev. C. 2004. V. 70. 024606.
5. *Gomes P. R. S. et al.* // Phys. Lett. B. 2006. V. 634. P. 356.
6. *Navin A. et al.* // Phys. Rev. C. 2004. V. 70. 044601.
7. *Bierman J. D. et al.* // Phys. Rev. C. 1993. V. 48. P. 319.

8. *Vandenbosch R.* // Ann. Rev. Nucl. Part. Sci. 1992. V. 42. P. 447.
9. *Danilin B. V. et al.* // Phys. Rev. C. 1991. V. 43. P. 2835.
10. *Ter-Akopian G. M. et al.* // Nucl. Phys. A. 2004. V. 734. P. 295.
11. *Beausang C. et al.* // Nucl. Instr. Meth. A. 1992. V. 313. P 37.
12. *Hauschild K. et al.* // Nucl. Instr. Meth. A. 2006. V. 560. P. 388.
13. *Tilquin I. et al.* // Nucl. Instr. Meth. A. 1995. V. 365. P. 446.
14. *Ter-Akopian G. M. et al.* // Phys. Rev. C. 1997. V. 55. P. 1146; see also http://159.93.28.88/flnr/dribs.html; http://159.93.28.88/dribs/publ.html.
15. *Baglin C. M.* // Nucl. Data Sheets. 2008. V. 109. P. 1103.
16. *Herman M. et al.* // Nucl. Data Sheets. 2007. V. 108. P. 2655.
17. *Dasso C. H., Landowne S.* // Comp. Phys. Commun. 1987. V. 46. P. 187.
18. *Zhukov M. V. et al.* // Phys. Rep. 1993. V. 231. P. 151.
19. *Koning A. et al.* www.talys.eu.

Received on December 2, 2011.